ORIGINAL ARTICLE

Recent flex power changes

Özge Gizem Esenbuğa[1] · André Hauschild[1] · Peter Steigenberger[1]

Abstract

The redistribution of the transmit power among different GPS signal components is called flex power, and it is implemented on modernized GPS satellites starting with Block IIR-M. The purpose of the flex power is to increase signal protection against jamming. It has been mostly active since the beginning of 2017 in different flex power modes and is visible in the carrier-to-noise density ratio (C/N_0) observations as stepwise changes. Especially after the beginning of 2020, the flex power modes changed frequently. We summarize these changes and study their impact on differential code biases (DCBs) which is 0.3 ns on average for L1 and L2 intra-frequency DCBs. The flex power is analyzed daily using C/N_0 measurements of the globally distributed GNSS observations network from January 1, 2020 until February 28, 2022. The flex power activation times are written into a dedicated block of the SINEX metadata format.

Keywords Flex power · GPS · Differential code biases

Introduction

Global positioning system (GPS) satellites transmit their signals from three different frequency bands, which are L1 at 1575.42 MHz, L2 at 1227.60 MHz and L5 at 1176.45 MHz. All satellites in the GPS constellation transmit the L1 C/A and P(Y) code as well as the L2 P(Y) code. In addition, the civil L2C signal and military M-code on L1 and L2 are provided by the newer satellite blocks starting with Block IIR-M. L5 signals are only available for satellites of Block IIF and Block III (Hegarty 2017; Johnston et al. 2017). Until January 2017, all GPS satellites transmitted their signals with constant power. After the modernization of GPS satellites, starting with Block IIR-M, it is possible to redistribute this power between the different signal components. The redistribution of the power between different GPS signal components is called flex power, and it is introduced as a remedy against jamming. This redistribution is necessary

as it is impossible to increase the power of all signal components. The redistribution of the power between different GPS signal components is observed on carrier-to-noise density ratio (C/N_0) observations as sub-daily stepwise changes. Currently, depending on the flex power mode, C/A and P(Y) code on L1 band and P(Y) code on L2 are observed to be affected by flex power on Block IIR-M and Block IIF satellites. Due to the adjustable power output property, the maximum value of the individual signal components of the Block IIR-M and Block IIF satellites can be exceeded, but this value is not expected to exceed −150 dBW. (IS-GPS-200M, 2021). It should be mentioned that flex power capability is also available on GPS Block III satellites; however, it has not been observed yet. Several studies have shown that flex power affects differential code biases and causes discontinuities up to 0.8 ns with an average of 0.4 ns (Steigenberger et al. 2018; Esenbuğa and Hauschild 2020; Esenbuğa et al. 2020).

The activation times of the flex power can change from day to day. Therefore, it is categorized under flex power modes. There are different modes of flex power, and some of them, until flex mode 4, have been discussed in the previously mentioned studies. First, the initial analysis of the impact of flex power on C/N_0 estimations is shown. A first flex power test campaign was conducted for only five days between September 7 and 12, 2010 (Jiménez-Baños et al. 2010). Next, early flex power changes from flex power mode

✉ Özge Gizem Esenbuğa
oezge.esenbuga@dlr.de

André Hauschild
andre.hauschild@dlr.de

Peter Steigenberger
peter.steigenberger@dlr.de

1 Deutsches Zentrum für Luft- und Raumfahrt, German Space Operations Center, 82234 Wessling, Germany

1 to mode 3 are studied (Steigenberger et al. 2018). In January 2017, flex power mode 1 started to be active for L1 C/A and P(Y) signals with one geographical center meaning that the flex power was activated if the elevation of a dedicated satellite was greater than 3 degrees with respect to the center point. Flex power mode 2 was first observed globally for a shorter amount of time in 2018, and after that, it was observed again in 2021. Flex mode 3 was active for a few days in 2018 and 2019. It has one geographical center similar to mode 1. Following this research, Esenbuğa and Hauschild (2020) analyzed the impact of the early flex power mode 1 on DCB estimations for L1 and L2 frequency bands and concluded that the impact of the flex power on L1 intra-frequency DCBs is more significant than L2 intra-frequency DCBs. Additionally, due to the impact of the ionosphere, L1–L2 inter-frequency biases is not as significant as intra-frequency DCBs. The effects of flex power mode 4 is studied, which was active from February 14 to April 12, 2020 (Esenbuğa et al. 2020). Different than flex power modes 1 and 3, this mode has, in fact, two geographical centers. Finally, Yang et al. (2022) developed a strategy to monitor flex power using machine learning and combined it with polynomial fitting.

After April 12, 2020, the flex power modes have been changed rather frequently. These changes in flex power have not yet been studied. Currently, the number of different flex power modes has increased to 9, and it is possible that it will increase even further. Additionally, up to flex power mode 4, it was possible to model the flex power changes with one or two geographical center points. After flex mode 5, the flex power implementations on GPS satellites have changed drastically. First, as the flex power mode changes frequently, it is not practical to define a rule stating the center points of the flex power. Second, it is not possible to look for a certain flex point center and model it for some flex power modes. Additionally, daily differences occur within the flex power modes, making the modeling more complicated.

Flex power is observed on C/N_0 observations as sub-daily stepwise changes. These observations are taken from International GNSS Service (IGS) (Johnston et al. 2017) network to identify the flex power activation times. Alternatively, high-gain antenna measurements can also be used to study flex power (Steigenberger et al. 2018). If the noise power is assumed to be constant, the C/N_0 observations can indicate the received signal strength. Although the C/N_0 observations from different stations are not directly comparable, stepwise changes in these measurements can be used to identify the flex power activation and deactivation times. A new algorithm, called the flex power detector (FPD), has been developed to identify the flex power activation times. This tool looks for stepwise changes in the C/N_0 observations and checks the number of occurrences within the network. If this number of occurrences reaches a certain value, it is defined as flex point activation or deactivation time. Additionally, in case the stepwise change in the C/N_0 observation is positive, the timestamp of it will be marked as flex point activation time for that satellite, and vice versa. The flex power activation times are written into a proposed extension of the SINEX metadata format. We first used FPD to retrieve the flex power activation and deactivation times and fed this information into estimations of DCBs. The time frame of this study is from January 1, 2020 until February 28, 2022.

High/low power mode detection

As the flex power changes are visible in the C/N_0 observations of geodetic GNSS receivers, it is possible to detect the time when satellites switch to high or low power. In case the satellite goes into high power, a stepwise jump is seen on the C/N_0 observations, and vice versa. Figure 1 depicts these stepwise variations for the station ALBH00CAN located in Victoria, Canada, which is part of the IGS network. The observations have a sampling of 30 s and show a drop in C/N_0 at ca. 11:20 h and an increase at 23:30 h.

Geodetic receivers use semi-codeless techniques to track the encrypted P(Y) code signals on L1 and L2 (Woo 2000). Therefore, C/N_0 observations of these signals are identical. Due to the limited sampling rate, short-term variations in the C/N_0 are not observable. If one uses a higher data rate, the result will look different. Figure 2 depicts the same drop occurring in Fig. 1 approximately at 11:20 h for 1 Hz data of different receiver types. Additionally, different receivers show different behaviors in the C/N_0 observations. Observations for Fig. 2 are taken from a geodetic antenna at Deutsches Zentrum für Luft- und Raumfahrt (DLR) Oberpfaffenhofen, Germany. Javad TRE-G3TH and Trimble NetR9 receivers show similar pattern with two stepwise drops in the C/N_0 observations of P(Y) code. On the other hand, the Septentrio PolaRx5 receiver shows rather a gradual change.

First, observations with 30 s data rate are screened using an elevation and C/N_0 threshold with 30 degrees and 30 dB-Hz. Since the beginning of 2020, the flex power is only affecting the P(Y) code on L1 and L2. Due to the nature of the semi-codeless tracking, C/N_0 observations of these bands are identical; therefore, stepwise changes on L2 P(Y) code of the C/N_0 observations over ca. 250 IGS stations are used to detect the activation and deactivation of the flex power times.

The measurements are processed, and the differences in C/N_0 observations between subsequent epochs are calculated to see the changes in C/N_0 measurements. Additionally, the average of C/N_0 observations is also calculated for the prior
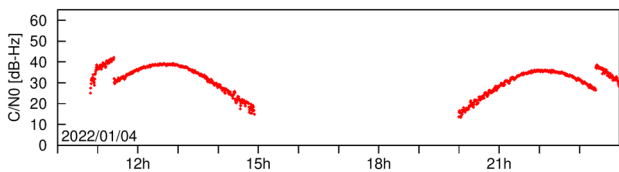
Fig. 1 C/N_0 observations on L1 and L2 P(Y) of satellite G072 from IGS station ALBH00CAN on January 4, 2022
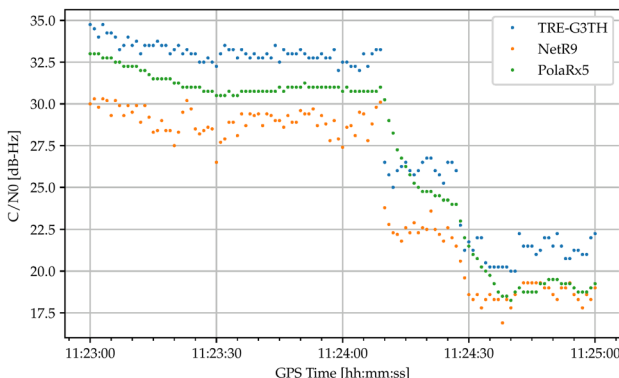

Fig. 2 P(Y) code C/N_0 observations of satellite G072 from a geodetic antenna at Oberpfaffenhofen/Germany with 1 Hz data rate on January 4, 2022

5 min with respect to the current epoch and 5 min later with respect to the next epoch. The difference between these averaged C/N_0 observations is also calculated along with the current and next epochs. This averaging aims to detect stepwise changes, in the case they are gradual with two or more steps. To differentiate these changes from noise, the stepwise change at the same epoch must occur at least from 20 different stations in the IGS network. If the stepwise change occurs at least as many as the predetermined value and it has a positive value, the corresponding satellite is going into high-power mode. If the step is in the other direction, it is marked as low-power mode.

The algorithm is tested each day from January 1, 2020 until February 28, 2022. In this time frame, the algorithm successfully detects the flex power activation and deactivation times except for the flex power mode 1. As this mode

has 2.5 dB changes on the C/N_0 measurements, it is currently not robust in differentiating the stepwise changes of flex power from noise. For flex power mode 1, a cone method is used to mark the high/low power modes. The cone method models the flex power mode 1 for most of the Block IIF satellites to go into high power in case their elevation is greater than 3° from its center at 41° E/37° N. More information on the cone method can be found in a study by Esenbuğa and Hauschild (2020).

Flex power modes

Flex power mode 1 was the main active mode from 2017 until February 2020. During this time period, flex power mode 2 was first observed in 2018. Later, this mode is observed again for 14 days in total in 2021. Finally, mode 3 was only active for a few days. Early flex power modes refer to the flex power modes 1–3. In February 2020, flex power modes started to change frequently. Using the high/low power detection method with the FPD algorithm mentioned above, flex power has been tested each day from January 1, 2020 until February 28, 2022. Figure 3 summarizes these flex power changes.

Early flex power modes

Flex power modes seen before 2020 for the first time are called early flex power modes. Three different flex power modes were detected on GPS Block IIR-M and Block IIF satellites by Steigenberger et al. (2018). In addition, mode 2 is detected again in 2021. These modes are summarized in Table 1. The second column includes the satellites that are included in the flex power mode. In case an entire satellite block is included in the flex power mode, the name of the satellite block is stated. Otherwise, the individual satellite vehicle numbers (SVN) are specified. The third column shows the activation time period of the flex mode in DOY/year format. There are some exceptional days with slight differences in high/low power patterns within the flex power mode 2. These days are mentioned under the fourth column. The fifth column shows the coverage of the flex power

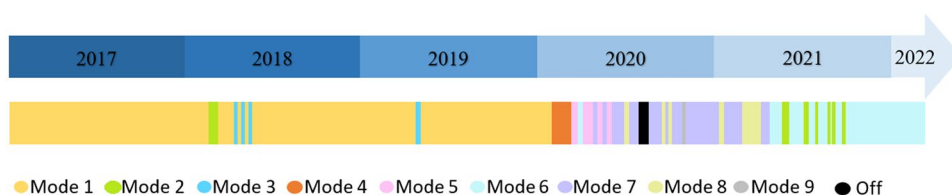**Fig. 3** Time evolution of flex power modes

Table 1 Summary of early flex power mode

Flex Power Mode	Satellites	Activation Period (DOY/Year)	Exceptions	Coverage	L1 C/A	L1 P(Y)	L2 P(Y)
Mode 1	Most Block-IIF satellites except for G070 & G073	027/2017–044/2020	–	Center at 41°E/37°N	+2.5 dB	+2.5 dB	–
Mode 2	IIR-M & IIF	103–107/2018 151–155/2021 254–257/2021 266–267/2021 296/2021 299/2021 320/2021	Exceptions on 266–267/2021, 296/2021, 299/2021, 320/2021	Global	–	+6 dB	+5 dB
Mode 3	IIR-M & IIF	117,121,124/2018 171–172/2019	–	Center at 115°W/40°N	–(2–3) dB	+9–11 dB	

mode and the latter columns show the characteristic stepwise changes in C/N_0 observations.

The regional flex power mode 1 was active from January 2017 until February 2020 on most Block IIF satellites for the L1 band. Flex power modes 2 and 3 were active for a rather shorter period of time on GPS Block IIR-M and Block IIF satellites (Steigenberger et al. 2018).

Recent flex power modes

In 2020, compared to the previous years, flex power changed more frequently. Some of these modes are first mentioned by Steigenberger et al. (2020). These flex power modes are denoted as recent flex power modes and summarized in Table 2. There is also one pattern observed for a day; however, it is excluded and not named as a new mode as it was active for less than three consecutive days. This is mentioned in Appendix 3. It should be mentioned that the individual L1 P(Y) and L2 P(Y) power changes can only be obtained from a high-gain antenna. As no high-gain observations are available to separate these measurements, only the sum of the L1 + L2 power change could be determined from C/N_0

measurements from the IGS network for flex power modes between 5 and 9.

Mode 4 was active from February 2020 until April 2020 on Block IIR-M and Block IIF satellites on L1 and L2 bands. Esenbuğa et al. (2020) detected and analyzed flex mode 4. This mode, like mode 1, can be modeled with the cone method but with two centers. The cone method marks Block IIR-M and Block IIF satellites in high power in case they have at least 3° elevation from one of the flex centers located at 37° E/35° N and 69° E/35° N. It is also possible to use the high/low power detection method. Figure 4 depicts flex mode 4 and it is obtained with this high/low power detection method on February 15, 2020. The crosses show the two centers of the flex power.

Flex power mode 5 looks similar to the previous flex power mode 4. However, it is more extended in the southward direction, which results in a reduced number of power transitions per day by ca. 25%. It is observed that on Block IIR-M and Block IIF satellites, there is a 9–11 dB power increase of L1 + L2 P(Y). This mode is first observed between April 13 and May 3, 2020. After that it is observed between May 9 to June 13, June 20 to 22, and July 3 to 6,

Table 2 Summary of recent flex power modes

Flex Power Mode	Satellites	Activation Period (DOY/Year)	Exceptions (DOY/Year)	Coverage	L1 C/A	L1 P(Y)	L2 P(Y)
Mode 4	IIR-M & IIF	045–103/2020	–	Center at 37°E/35°N & 69°E/35°N	–	+6 dB	+5 dB
Mode 5	IIR-M & IIF	104–124/2020 130–165/2020 172–174/2020 185–188/2020	–		–		+9–11 dB
Mode 6	IIR-M & IIF	125–129/2020 137–150/2021 156–253/2021 258–265/2021 268–295/2021 297–298/2021 300–319/2021 321/2021–059/2022	–	Between longitudes 155°E & 30°W	–		+9–11 dB
Mode 7	IIR-M & IIF	166–171/2020 175–184/2020 189–215/2020 235–256/2020 275–292/2020 298–299/2020 310–320/2020 326/2020–011/2021 016–064/2021 122–136/2021	192–198/2020	Center at 111°W/33°N & 33°E/34°N & 70°E/35°N	–		+9–11 dB
Mode 8	IIR-M & IIF	216–234/2020 293–297/2020 300–309/2020 012–015/2021 065–121/2021	–	Center at 109°W/32°N & 70°E/35°N	–		+9–11 dB
Mode 9	IIR-M & IIF	321–325/2020	–	Center at 76°W/41°N & 70°E/35°N	–		+9–11 dB

2020. In total, this mode was observed for 64 days. An illustration of flex mode 5 is depicted in Fig. 5.

As illustrated in Fig. 6, flex power mode 6 is rather different than the other modes. It is activated between longitudes 155° E and 30° W. Similar to mode 5, it results in 9–11 dB power increase of L1 + L2 P(Y) on Block IIR-M and Block IIF satellites. This mode has first been observed on May 4 until May 8, 2020. This mode was active for 4 days in 2020; however, it was observed for 215 days in 2021. In 2022, this mode is observed for all of the 59 days tested, meaning that this is the only flex power mode that has been observed in 2022.

Different than the other flex power modes, flex power mode 7 has three different centers located at 111° W/33° N, 33° E/34° N, and 70° E/35° N, see Fig. 7. Similar to the previous modes, it is observed that on Block IIR-M and Block IIF satellites, there is a 9–11 dB power increase in the sum of L1 and L2 P(Y). It was observed for the first time on June 14, 2020. It lasted 6 days and ended on June 19, 2020.

However, after that it was observed quite frequently. The longest duration of its activation is from November 21, 2020 until January 11, 2021. Overall this mode was observed in total for 137 days in 2020. For 2021, it is observed for 75 days. In addition, flex mode 7 has visible exceptions between July 10 and 16, 2020. However, it is still included in this mode to keep the flex power modes as compact as possible. The exceptions include SVNs G062, G063, G065, G066, G071, and G072. It is observed that these satellites go on high power later that it normally should when it is compared to the typical flex mode 7.

Similar to flex power mode 4, flex power mode 8 has two centers located at 109° W/32° N and 70° E/35° N shown in Fig. 8. On Block IIR-M and Block IIF satellites, it causes 9–11 dB power increase on L1 + L2 P(Y). This mode was observed first between August 3 and 21, 2020. After that it was observed again 2020 between October 19 and 23. Hence, this mode was active for 34 days in 2020. For 2021,

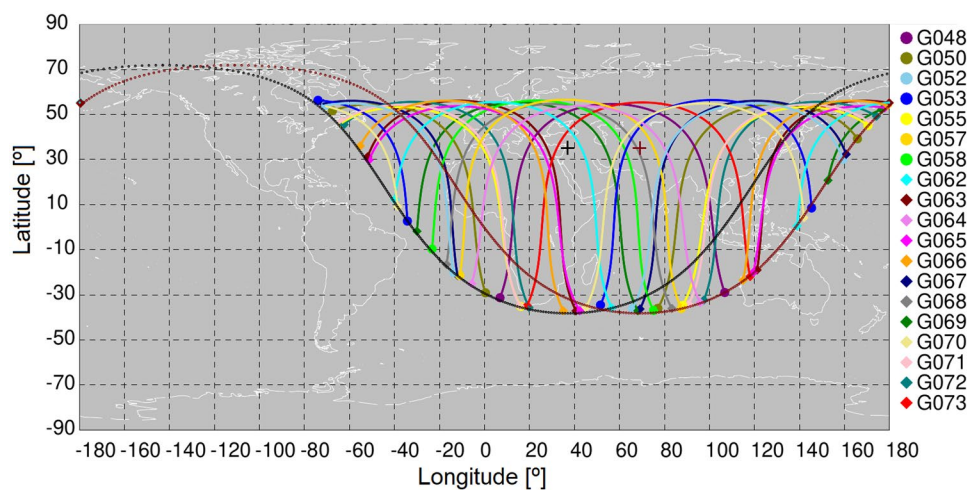**Fig. 4** Example day for the flex mode 4 on February 15, 2020 with two centers symbolized as crosses

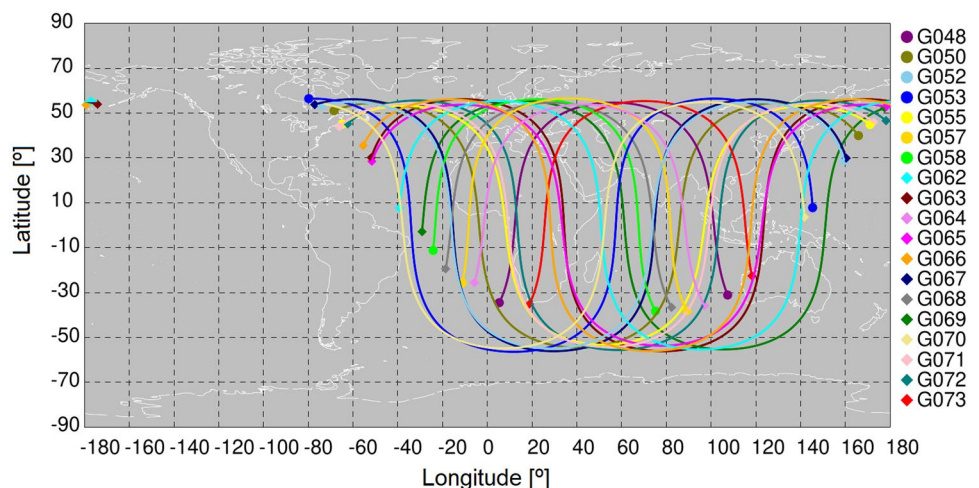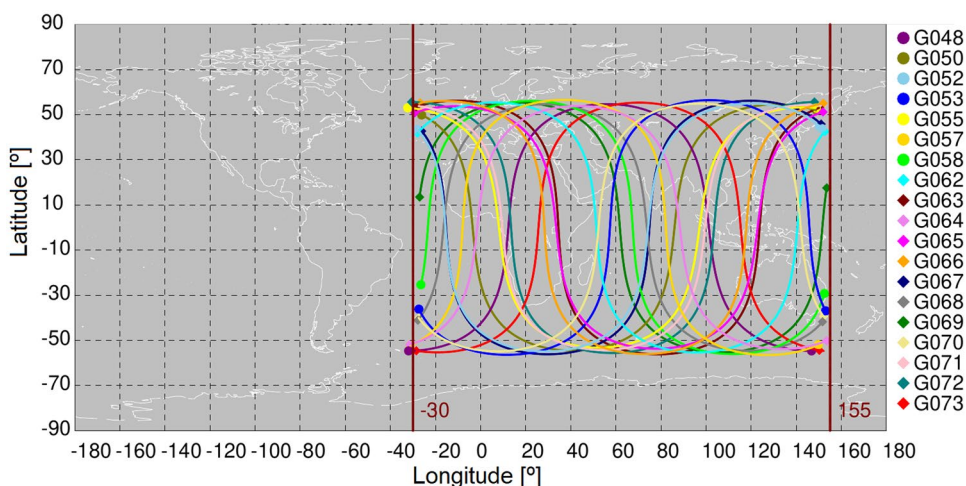**Fig. 5** Example day for the flex mode 5 on April 14, 2020

Fig. 6 Example day for the flex mode 6 on May 5, 2020

flex mode 8 was observed for 61 days in total. It has not yet been observed in 2022.

Flex power mode 9 was centralized at 76° W/41° N and 70° E/35° N and it is shown in Fig. 9. This mode results in a 9–11 dB power increase in the sum of L1 and L2 P(Y) codes for GPS Block IIR-M and Block IIF satellites. It was active for a very short time period between November 16 and 20, 2020. Therefore, it is likely to assume that this mode was active for some testing purposes.

Flex power impact on DCBs

Previous studies show that flex power affects the estimation of the differential code biases (DCBs) (Steigenberger et al. 2018; Esenbuğa and Hauschild 2020; Esenbuğa et al. 2020). The magnitude of this effect differs for each satellite and each mode. Flex power is considered for estimations of DCBs. To do this, two different DCBs for each pseudorange observation combination having flex power activation throughout the day are estimated. This results in two different DCBs for each combination when the flex power is on and off. Therefore, these biases are named "normal" and "flex" DCBs, respectively.

The impact of the flex power is not notable for interfrequency DCBs due to the influence of the ionosphere. However, this effect can be significant for intra-frequency DCBs. Therefore, intra-frequency DCBs on L1 and L2 bands are estimated. To identify DCBs, two observation codes are used; each of them consists of three characters. The estimated DCBs are C1C–C1W, C2W–C2L, C2W–C2S, and C2W–C2X. The first character in the observation code, which is in this case 'C', shows that it is a pseudorange observation. The second character is a number, and it stands for the band. Finally, the last character shows the channel or the tracking mode of the signal. C1C is provided via C/A code on L1, whereas C1W and C2W stand for semi-codeless tracking of the encrypted

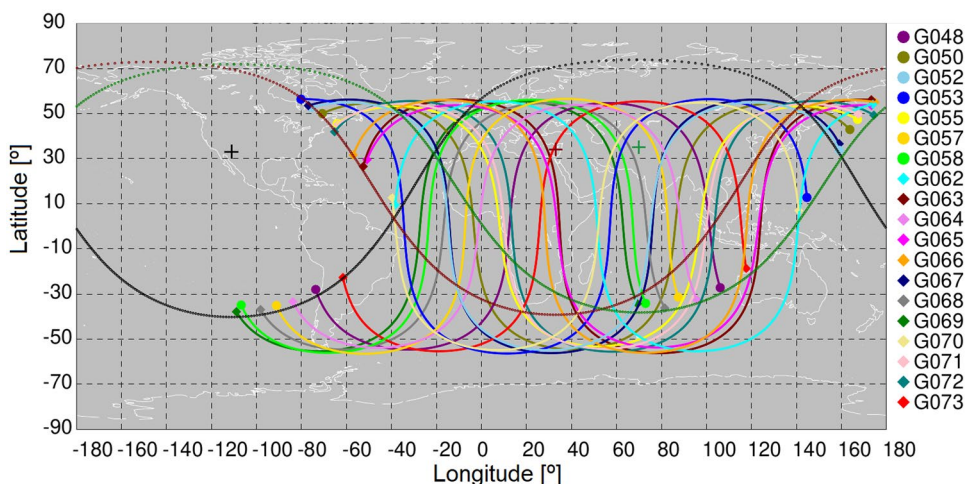**Fig. 7** Example day for the flex mode 7 on June 15, 2020 with three centers symbolized as crosses

Fig. 8 Example day for the flex mode 8 on August 4, 2020 with two centers symbolized as crosses
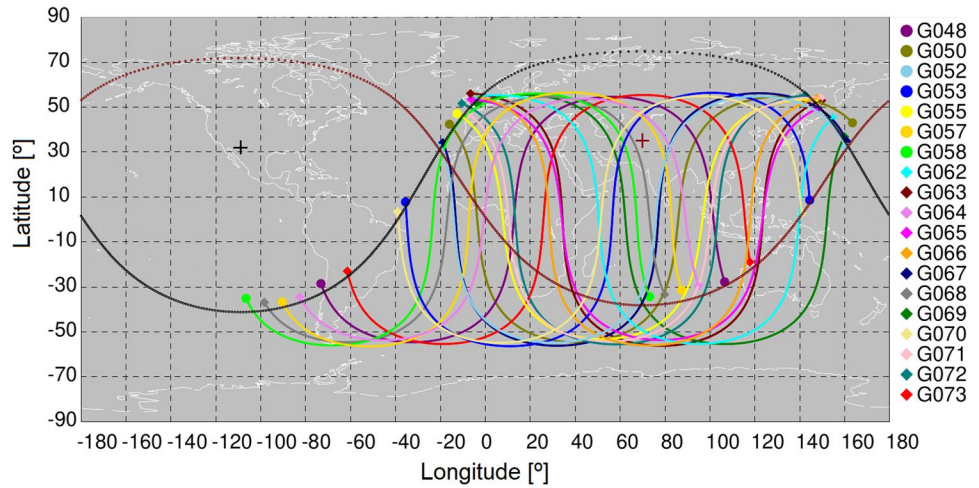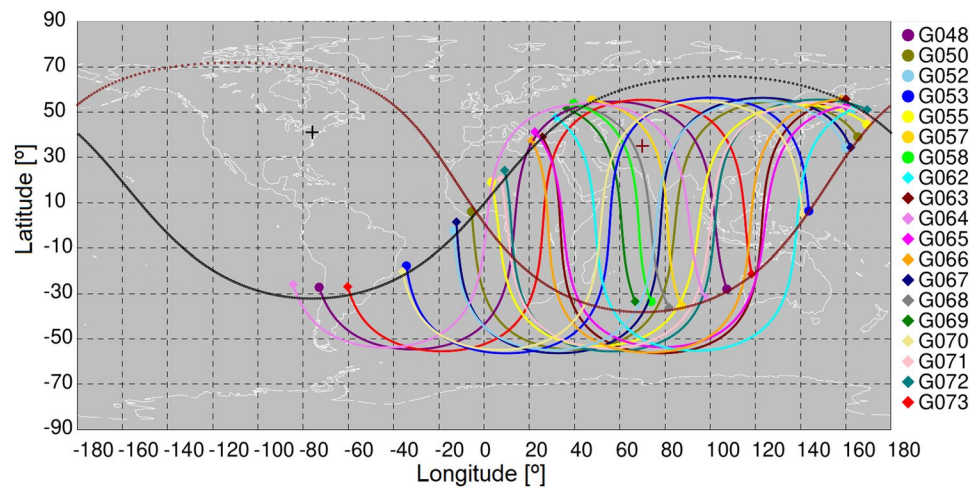

Fig. 9 Example day for the flex mode 9 on November 16, 2020 with two centers symbolized as crosses

P(Y) code on L1 and L2, respectively. C2L, C2S and C2X are provided via different signal components of the L2C pseudorange, which are, respectively, L, M, and mixed M + L codes (IGS RINEX Working Group and RTCM-SC104 2018). The normal and flex C1C–C1W DCBs on L1 band are, depicted in Figs. 10 and 11, respectively. It should also be mentioned that the standard deviations of these DCB estimations are between 0.03 and 0.05 ns.

As the normal and flex DCBs are mostly stable in the same mode, the average of DCBs on L1 band for each mode is listed in Table 3. The absolute difference between averaged normal and flex C1C–C1W DCBs is depicted in Fig. 12 to show the impact of the corresponding flex power mode.

Both Fig. 12 and Table 3 show that except for mode 1 the flex DCBs are similar to each other for the same satellite in different flex power modes. The normal DCBs have

similar values for all of the modes. Except for mode 1, the flex power affects the L1 intra-frequency DCBs by a magnitude of 0.3 ns on average, ranging from 0.82 ns with a maximum for G073 and 0.01 ns with a minimum for G068. For mode 1, this impact on C1C–C1W DCBs is 0.4 ns on average with a maximum of 0.91 ns for G067 and 0.01 ns with a minimum for G066.

For L2 intra-frequency C2W–C2L DCBs, the impact of flex power is analyzed. It should be noted that C2L signal is mostly provided by Septentrio PolaRx5 receivers, whereas C2W observations are available by almost all receivers within the network. Flex power mode 1 is not included as it does not affect any power changes on L2. The maximum value is 0.68 ns for satellite G050. The minimum value is 0.01 ns for satellites G052 and G064. It should be noted that the flex power impact is rather stable on average for
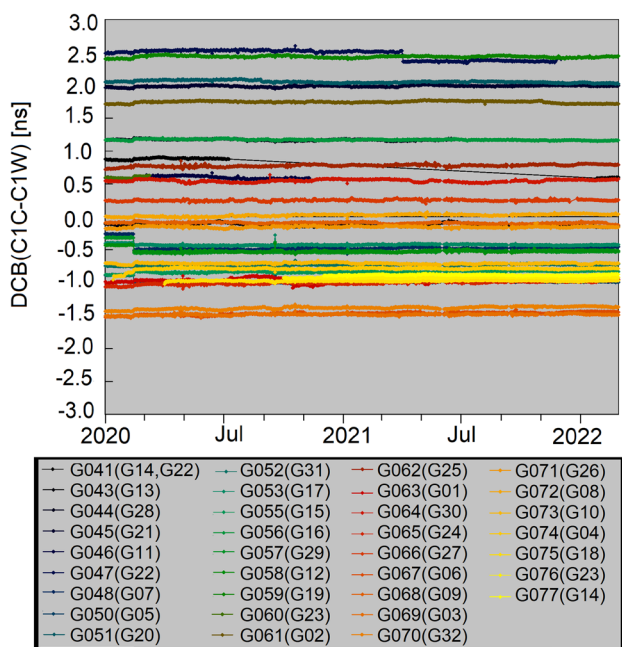
Fig. 10 Normal C1C–C1W DCBs over the estimated time period from January 1, 2020 until February 28, 2022
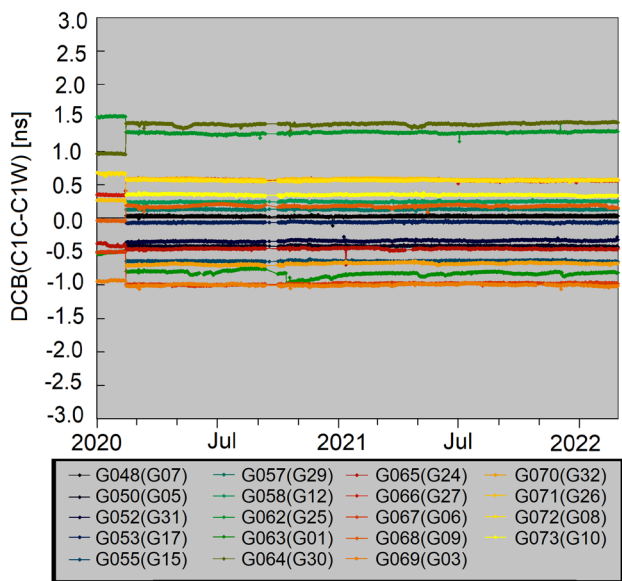

Fig. 11 Flex C1C–C1W DCBs over estimated time period from January 1, 2020 until February 28, 2022

each satellite within the mode change. The impact of the flex power is depicted in Fig. 13. The impact of flex power on L2 C2W–C2L is 0.3 ns on average for all the flex power modes from mode 4 to 9.

Similar to the C2W–C2L, the impact of the flex power on C2W–C2S DCBs is shown in Fig. 14. It should be noted that C2L observations are provided by Leica receivers within the network, which is quite limited. On the other hand, C2W signal is available by almost all receivers within the network. The range of the impact of flex power for DCBs is between 0.63 ns for G067 and 0.01 ns for G068. It should also be noted that the average impact of C2W–C2L and C2W–C2S is the same, however different for each satellite. The impact of C2W–C2S DCBs is between 0.2 and 0.3 ns on average. For flex power mode 4, it has an impact of 0.2 ns on average, and it ranges from 0.58 ns for G067 to 0.01 for G048 and G068.

Finally, the impact of flex power on C2W–C2X DCBs is analyzed. C2X observations are provided mostly by Trimble and Javad receivers within the IGS network. Different than other modes, the flex power impact differs between each mode for each satellite. It takes its maximum value of 0.44 ns for satellite G067 and 0.01 ns for satellite G048. This is depicted in Fig. 15. The impact of C2W–C2X DCBs is 0.2 ns for all flex power modes.

Conclusion

Flex power activity is analyzed daily for a 2 years period starting on the first calendar day of 2020 until the end of February 2022. Nine different flex power modes are observed until the end of February 2022. Most of them occurred in 2020 and 2021. For 2022, only mode 6 has been observed so far. It should also be mentioned that flex power is currently activated for Block IIR-M and Block IIF satellites and has not yet been observed in Block III satellites.

The daily changes of the flex power are documented for these days in the dedicated SATELLITE/FLEX_POWER block of the SINEX metadata format described in Appendix 1 and shown in a video Appendix 2. In addition to these modes, there is also one exceptional day on September 18, 2020. As it is not observed for at least three subsequent days, it is not called a new flex power mode. This can be seen

Table 3 Average of normal and flex DCBs for each flex power mode

| SVN	Block	C1C–C1W normal DCBs (ns)							C1C–C1W flex DCBs (ns)						
		Flex power mode							Flex power mode						
		1	4	5	6	7	8	9	1	4	5	6	7	8	9
G048	IIR-M	− 0.40	− 0.61	− 0.57	− 0.46	− 0.49	− 0.48	− 0.48	–	− 0.32	− 0.30	− 0.20	− 0.23	− 0.23	− 0.24
G050		− 1.03	− 1.11	− 1.09	− 0.96	− 1.00	− 0.99	− 1.00	–	− 0.78	− 0.75	− 0.65	− 0.68	− 0.68	− 0.67
G052		− 0.89	− 0.86	− 0.83	− 0.71	− 0.75	− 0.73	− 0.73	–	− 0.71	− 0.67	− 0.57	− 0.60	− 0.60	− 0.60
G053		− 0.54	− 0.54	− 0.52	− 0.40	− 0.44	− 0.42	− 0.43	–	− 0.43	− 0.39	− 0.29	− 0.32	− 0.32	− 0.33
G055		− 1.02	− 0.96	− 0.93	− 0.81	− 0.85	− 0.84	− 0.84	–	− 1.00	− 0.97	− 0.88	− 0.90	− 0.91	− 0.89
G057		− 0.46	− 0.66	− 0.63	− 0.50	− 0.54	− 0.54	− 0.53	–	− 0.23	− 0.20	− 0.10	− 0.13	− 0.13	− 0.15
G058		− 0.57	− 0.65	− 0.61	− 0.49	− 0.54	− 0.53	− 0.51	–	− 0.12	− 0.09	0.01	− 0.02	− 0.02	− 0.04
G062	IIF	0.60	0.66	0.68	0.79	0.77	0.79	0.80	1.28	0.93	0.94	1.03	1.02	1.01	1.00
G063		− 1.13	− 1.08	− 1.06	− 0.95	− 0.99	− 0.96	− 1.04	− 0.75	− 1.15	− 1.14	− 1.07	− 1.10	− 1.09	− 1.20
G064		0.40	0.45	0.45	0.56	0.55	0.55	0.56	0.73	1.06	1.06	1.17	1.14	1.14	1.12
G065		− 1.20	− 1.14	− 1.11	− 0.97	− 1.02	− 1.00	− 0.99	− 0.64	− 0.82	− 0.79	− 0.70	− 0.71	− 0.73	− 0.73
G066		0.10	0.14	0.16	0.28	0.24	0.27	0.27	0.11	0.22	0.26	0.33	0.32	0.31	0.31
G067		− 1.66	− 1.60	− 1.58	− 1.44	− 1.48	− 1.46	− 1.48	− 0.75	− 1.35	− 1.33	− 1.22	− 1.25	− 1.25	− 1.27
G068		− 0.23	− 0.20	− 0.17	− 0.06	− 0.10	− 0.10	− 0.09	− 0.28	− 0.19	− 0.15	− 0.05	− 0.08	− 0.09	− 0.11
G069		− 1.65	− 1.61	− 1.57	− 1.46	− 1.49	− 1.48	− 1.48	− 1.18	− 1.37	− 1.32	− 1.23	− 1.26	− 1.26	− 1.30
G070		− 1.58	− 1.52	− 1.48	− 1.37	− 1.39	− 1.38	− 1.39	–	− 1.06	− 1.02	− 0.92	− 0.94	− 0.94	− 0.95
G071		− 0.31	− 0.26	− 0.24	− 0.14	− 0.16	− 0.14	− 0.13	0.03	0.23	0.26	0.34	0.32	0.32	0.32
G072		− 0.15	− 0.11	− 0.09	0.06	0.02	0.04	0.04	0.43	0.22	0.24	0.33	0.30	0.30	0.28
G073		− 0.86	− 0.82	− 0.79	− 0.70	− 0.71	− 0.71	− 0.70	–	0.00	0.03	0.11	0.09	0.09	0.07
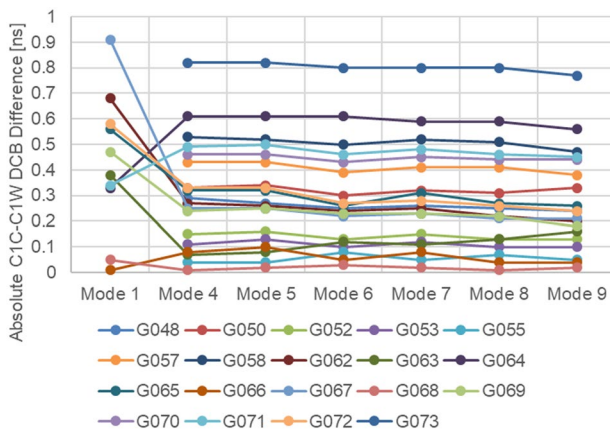
Fig. 12 Absolute differences between averaged flex DCBs and averaged normal DCBs of C1C–C1W
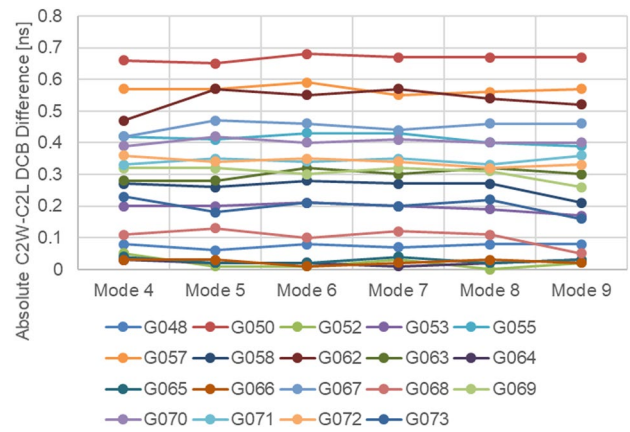

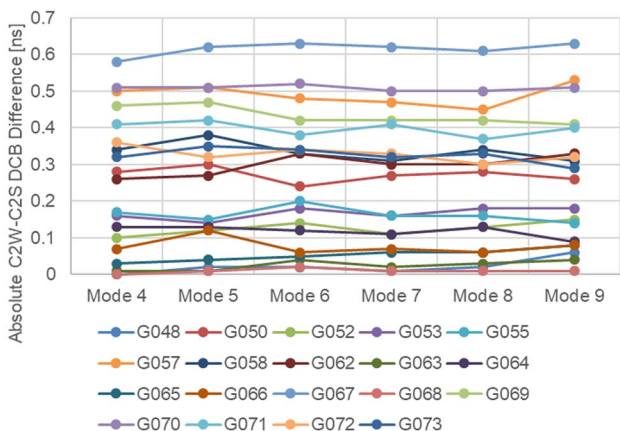**Fig. 13** Absolute differences between averaged flex DCBs and averaged normal DCBs of C2W–C2L

Fig. 14 Absolute differences between averaged flex DCBs and averaged normal DCBs of C2W–C2S
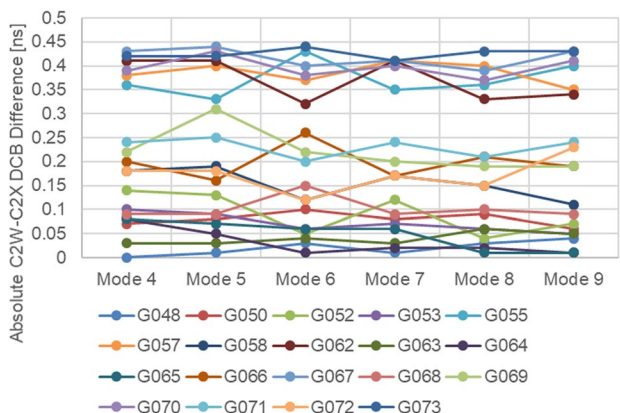

Fig. 15 Absolute differences between averaged flex DCBs and averaged normal DCBs of C2W–C2X

in Appendix 2 in the video or Appendix 3. The analysis shows that the impact of the flex power on L1 and L2 intra-frequency DCBs is approximately 0.3 ns on average on both L1 and L2 intra-frequency DCBs. For L1 intra-frequency DCBs, this can reach up to 0.9 ns; on L2, this value is 0.7 ns. As the averaged standard deviation is approximately between 0.03 ns and 0.05 ns for these DCB estimations, it can be relevant for high-accuracy DCB estimations.

Appendix 1. Proposed flex power SINEX format

In this section, a dedicated SATELLITE/FLEX_POWER block of the SINEX metadata format (Steigenberger and Montenbruck 2022) is proposed. This block contains the timestamps for GPS satellites going into high or low power mode. The proposed format includes 4 columns in total. These columns are the space vehicle number (SVN) as a unique identifier, starting timestamp, ending timestamp, and flex power state. In case the satellite goes into the high-power state, flex power state will show "ON". This will be "OFF" for a low power state. An example of the proposed block is shown in Fig. 16.

The naming of the proposed format is defined as follows. Note that placeholders YYYY, DDD, HH, MM are the current year, day of the year, hour and minute, respectively.

- DLR0OPSSNX_YYYYDDDHHMM_01D_00U_FLX. SNX

  This file contains daily observations for 1 day of the flex power timestamps in flex power SINEX format.
- DLR0OPSSNX_YYYYDDDHHMM_30D_00U_FLX. SNX

  This file contains daily observations for 30 days of the flex power timestamps in flex power SINEX format.

Appendix 2. Flex power since 2020

C/N_0 measurements of a globally distributed network are used to analyze daily flex power changes. These daily results are merged into a video file to summarize the flex power changes.

Appendix 3. Exception days

On September 18, 2020 an irregularity was observed in terms of the pattern of the flex power. As it only occurred for a day, it is not counted as a new mode. This was the only irregularity observed in 2020 as depicted in Fig. 17.
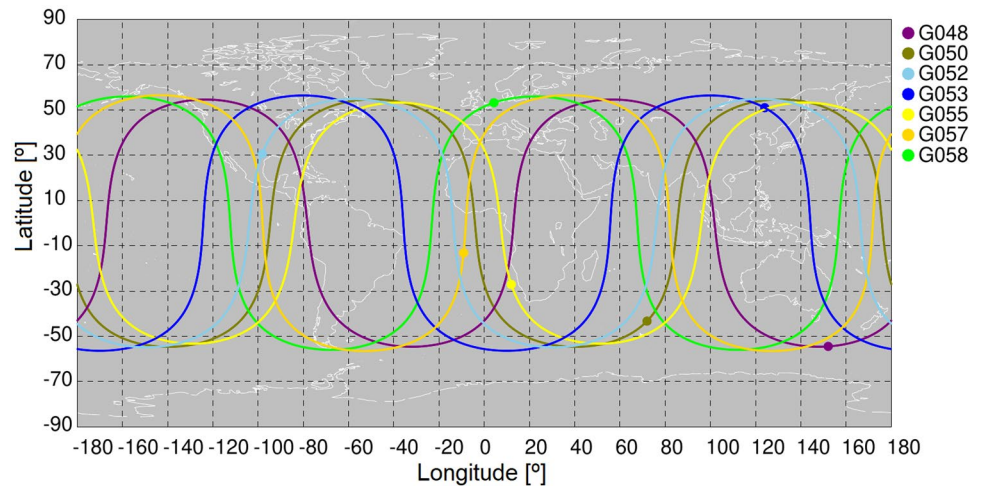
Fig. 16 An example of the proposed flex power SINEX format

```
%=SNX 2.02 DLR 21:224:31335 DLR 21:002:00000 21:003:00000 P 00000 0
*-------------------------------------------------------------------------------
*
+SATELLITE/FLEX_POWER
*
*SVN_ Start_____ End_____ Flex_Power Comment_____
*
 G043 2021:002:00000 2021:003:00000 OFF
 G044 2021:002:00000 2021:003:00000 OFF
 G045 2021:002:00000 2021:003:00000 OFF
 G046 2021:002:00000 2021:003:00000 OFF
 G047 2021:002:00000 2021:003:00000 OFF
 G048 2021:002:00000 2021:002:10080 OFF
 G048 2021:002:10080 2021:002:52560 ON
 G048 2021:002:52560 2021:003:00000 OFF
 G050 2021:002:00000 2021:002:33120 OFF
 G050 2021:002:33120 2021:002:82800 ON
 G050 2021:002:82800 2021:003:00000 OFF
 G051 2021:002:00000 2021:003:00000 OFF
 G052 2021:002:00000 2021:002:28800 ON
 G052 2021:002:28800 2021:002:64800 OFF
 G052 2021:002:64800 2021:003:00000 ON
 G053 2021:002:00000 2021:002:14400 OFF
 G053 2021:002:14400 2021:002:66960 ON
 G053 2021:002:66960 2021:003:00000 OFF
 G055 2021:002:00000 2021:002:05760 ON
 G055 2021:002:05760 2021:002:42480 OFF
 G055 2021:002:42480 2021:003:00000 ON
 G056 2021:002:00000 2021:003:00000 OFF
 G057 2021:002:00000 2021:002:02910 ON
 G057 2021:002:02910 2021:002:46080 OFF
 G057 2021:002:46080 2021:003:00000 ON
 G058 2021:002:00000 2021:002:34560 OFF
 G058 2021:002:34560 2021:002:77790 ON
 G058 2021:002:77790 2021:003:00000 OFF
 G059 2021:002:00000 2021:003:00000 OFF
 G061 2021:002:00000 2021:003:00000 OFF
 G062 2021:002:00000 2021:002:21630 ON
 G062 2021:002:21630 2021:002:56190 OFF
 G062 2021:002:56190 2021:003:00000 ON
 G063 2021:002:00000 2021:002:05790 OFF
 G063 2021:002:05790 2021:002:55470 ON
 G063 2021:002:55470 2021:003:00000 OFF
 G064 2021:002:00000 2021:002:14430 OFF
 G064 2021:002:14430 2021:002:56910 ON
 G064 2021:002:56910 2021:003:00000 OFF
 G065 2021:002:00000 2021:002:10830 ON
 G065 2021:002:10830 2021:002:46830 OFF
 G065 2021:002:46830 2021:003:00000 ON
 G066 2021:002:00000 2021:002:42510 ON
 G066 2021:002:42510 2021:002:79230 OFF
 G066 2021:002:79230 2021:003:00000 ON
*
-SATELLITE/FLEX_POWER
*
*-------------------------------------------------------------------------------
%ENDSNX
```

Fig. 17 High power pattern observed on September 18, 2020

Declarations

References

Esenbuğa ÖG, Hauschild A (2020) Impact of flex power on GPS Block IIF differential code biases. GPS Solut 24(4):91. https://doi.org/10.1007/s10291-020-00996-x

Esenbuğa ÖG, Hauschild A, Steigenberger P (2020) Impact of GPS flex power on differential code bias estimation for Block IIR-M and IIF satellites. In: Proceedings of ION GNSS+ 2020, pp 2922–2930. https://doi.org/10.33012/2020.17634

Hegarty CJ (2017) The global positioning system. In: Teunissen PJG, Montenbruck O (eds) Springer handbook of global navigation satellite systems. Springer Handbooks, Cham, pp 197–218. https://doi.org/10.1007/978-3-319-42928-1_7

IGS RINEX Working Group and RTCM-SC104 (2018) RINEX the receiver independent exchange format version 3.04. https://files.igs.org/pub/data/format/rinex304.pdf

IS-GPS-200M (2021) NAVSTAR GPS space segment/navigation user segment interfaces. https://www.gps.gov/technical/icwg/IS-GPS-200M.pdf

Jiménez-Baños D, Perelló-Gisbert J, Crisci M (2010) The measured effects of GPS flex power capability collected on sensor station data. In: 5th ESA workshop on satellite navigation technologies and european workshop on GNSS signals and signal processing (NAVITEC), pp 1–6. https://doi.org/10.1109/NAVITEC.2010.5708073

Johnston G, Riddell A, Hausler G (2017) The International GNSS Service. In: Teunissen PJG, Montenbruck O (eds) Springer handbook of global navigation satellite systems. Springer Handbooks, Cham, pp 967–982

Noll C (2010) The crustal dynamics data information system: a resource to support scientific analysis using space geodesy. Adv Space Res 45(12):1421–1440. https://doi.org/10.1016/j.asr.2010.01.018

Steigenberger P, Montenbruck O (2022) IGS satellite metadata file description, Version 1.00, December 13, 2022. https://doi.org/10.57677/metadata-sinex

Steigenberger P, Thölert S, Montenbruck O (2018) Flex power on GPS Block IIR-M and IIF. GPS Solut 23(1):8. https://doi.org/10.1007/s10291-018-0797-8

Steigenberger P, Thölert S, Esenbuğa ÖG, Hauschild A, Montenbruck O (2020) The new flex power mode: from GPS IIR-M and IIF satellites with extended coverage area. Inside GNSS 15:52–56

Woo K (2000) Optimum semicodeless carrier-phase tracking of L2. J Ins Navig 47(2):82–99

Yang X, Liu W, Huang J, Xiao W, Wang F (2022) Real-time monitoring of GPS flex power based on machine learning. GPS Solutions. https://doi.org/10.1007/s10291-022-01257-9

Publisher's Note Springer Nature remains neutral with regard to jurisdictional claims in published maps and institutional affiliations.

Özge Gizem Esenbuğa received her B.S. degree in geomatics engineering from Istanbul Technical University in 2016, and an M.S. degree in earth-oriented space science and technology (ESPACE) from the Technical University of Munich in 2018. After her graduation, she joined the German Space Operations Center (GSOC) at DLR. Her research interest is in GNSS data analysis, particularly differential code bias determination of GNSS satellites and ionosphere modeling. She also works on projects for interface development for GNSS data visualization.

André Hauschild is a scientific staff member at DLR's German Space Operations Center (GSOC) and focuses on precise real-time clock estimation for GNSS satellites and multi-GNSS processing using new and modernized satellite navigation systems. André is also involved in projects with space-borne GNSS for scientific applications on satellites and rockets. Since 2014, he has been a member of Eumetsat's Radio Occultation Science Advisory Group and has led the International GNSS Service (IGS) real-time working group since 2019. He is the 2019 recipient of the Institute of Navigation's Tycho Brahe Award.

Peter Steigenberger received his master and Ph.D. degrees in Geodesy from Technische Universität München (TUM) in 2002 and 2009, respectively. Currently, he is a senior researcher at DLR's German Space Operations Center (GSOC). His research interests focus on GNSS data analysis, particularly the precise orbit and clock determination of GNSS satellites and the evolving navigation systems of Galileo, BeiDou, and QZSS.